

Research Article

Exploring the Use of Fengyun-3 Meteorological Satellite for Monitoring Sea Ice to Provide Services for Polar Navigation

Lixiong Chen^{*} , Dongkui Wu , Chun Shen 

Merchant Marine College, Shanghai Maritime University, Shanghai, China

Abstract

This paper explores the feasibility and effectiveness of using the Fengyun-3 meteorological satellite to monitor sea ice, providing services for ships navigating in polar regions. Firstly, it analyzes the impact of Arctic sea ice changes on ship navigation and the importance of sea ice monitoring in route planning. Next, it provides a detailed introduction to the data sources and processing methods of the Fengyun-3 satellite, including radiometric calibration, geometric correction, image registration, and cropping. Subsequently, it discusses the characteristics of sea ice in the visible spectrum and successfully extracts sea ice information using MERSI-II data with land, cloud, and seawater masking techniques. The study indicates that the comprehensive use of multi-spectral data and other observation methods can significantly enhance sea ice monitoring capabilities. In the future, integrating more advanced technologies is expected to achieve refined identification and short-term prediction of sea ice movement, thereby providing more scientific and efficient support for ships navigating in polar regions, enhancing navigation safety and efficiency, and offering a scientific basis for the development of Arctic shipping routes.

Keywords

Sea Ice Monitoring, Fengyun-3 Satellite, Polar Navigation, Remote Sensing Technology

1. Introduction

With the intensification of global climate change, the Arctic region is experiencing rapid changes in sea ice. The continuous reduction in summer sea ice extent and the prolonged melting season present more opportunities and conveniences for commercial shipping. This change makes it possible to open new shipping routes in high-latitude areas and extends the shipping period for these routes. However, compared to low-latitude seas, the climate and marine environment in the Arctic are more complex, posing extremely harsh and complicated conditions for vessels navigating in polar regions, which puts navigation safety under severe test [1, 2]. The presence of sea ice can create obstacles and risks for vessels,

such as collisions and entrapment [3]. Therefore, sea ice monitoring is essential for route planning. Real-time monitoring and forecasting of sea ice distribution and evolution are critical for selecting safe routes, avoiding ice obstructions, and steering clear of hazardous areas. Ships need to meet higher technical and safety requirements to engage in shipping activities in the Arctic region. Accurate monitoring and forecasting of sea ice distribution and evolution is a key step. In summary, the changes in Arctic sea ice present opportunities for commercial shipping but also increase navigation safety risks. Thus, sea ice monitoring is crucial for route planning and vessel safety [4, 5].

^{*}Corresponding author: chenlixiong2002@163.com (Lixiong Chen)

Received: 5 September 2024; **Accepted:** 26 September 2024; **Published:** 10 October 2024



Copyright: © The Author (s), 2024. Published by Science Publishing Group. This is an **Open Access** article, distributed under the terms of the Creative Commons Attribution 4.0 License (<http://creativecommons.org/licenses/by/4.0/>), which permits unrestricted use, distribution and reproduction in any medium, provided the original work is properly cited.

In selecting data sources for sea ice monitoring, due to the Arctic's unique geographical position and harsh natural conditions, on-site observations are primarily conducted using ships, buoys, and observation stations. However, these methods provide sparse spatial distribution of data, making it difficult to achieve continuous temporal and spatial monitoring of sea ice [6]. To overcome this issue, space remote sensing technology has been widely applied for tracking Arctic sea ice in recent years. Among these, microwave sensors have become the primary data source for sea ice monitoring due to their all-weather and all-time capabilities. Passive microwave radiometers (such as SSM/I (Special Sensor Microwave/Imager) and AMSR-2 (Advanced Microwave Scanning Radiometer-2)) and active microwave sensors (such as scatterometers and SAR (Synthetic Aperture Radar)) are commonly used as microwave sensors. Microwave radiometers and scatterometers have short revisit cycles and lower spatial resolution, mainly used for large-scale sea ice monitoring. The polar sea ice remote sensing monitoring products released by international research institutions such as NSIDC (National Snow and Ice Data Center), IFREMER (French Research Institute for the Exploitation of the Seas), and OSI-SAF (the Ocean and Sea Ice Satellite Application Facility) typically utilize microwave scatter/radiometer data; however, due to the lower resolution, these sensors struggle to monitor complex sea ice conditions in local areas at fine scales [7-9]. SAR data have high spatial resolution, but generally have a narrow swath and long revisit cycle, making it unsuitable for short-term (e.g., daily) monitoring. Additionally, sea ice monitoring using microwave data relies on sea ice brightness temperature or backscattering signals, and summer melting of sea ice alters brightness temperature and backscatter coefficients, limiting the availability of microwave data for summer sea ice monitoring [10]. Optical data are less frequently used in sea ice monitoring studies due to cloud cover impacts. However, the spectral information and spatial texture information provided by optical data is less affected by summer melting [11]. Furthermore, certain optical sensors (such as MODIS (Moderate-resolution Imaging Spectroradiometer)) have advantages such as wide swath, high spatial resolution, and short revisit cycles. Utilizing daily multi-scene overlapping images can reduce cloud impacts and serves as a better data source for daily summer sea ice monitoring in local areas (e.g., near shipping routes) [12].

The Fengyun-3 meteorological satellite, as China's latest generation of near-polar orbit observation satellites, has high-frequency and high-resolution observation capabilities, providing new avenues for sea ice monitoring. The purpose of this paper is to explore the feasibility and effectiveness of monitoring sea ice using Fengyun-3 satellites to support vessel navigation in polar regions. This includes discussing the methods and technologies for sea ice monitoring and forecasting using Fengyun-3 satellite data and exploring its application potential in polar vessel navigation. Through this research, we aim to provide high-resolution sea ice infor-

mation for vessels navigating in polar regions, thereby supporting the development and utilization of Arctic shipping routes. Utilizing Fengyun-3 meteorological satellite data for sea ice monitoring enriches the low-resolution inversion products, providing more scientific and efficient support for the planning of Arctic shipping routes and vessel navigation [13, 14].

2. Data, Models, and Analysis Methods

2.1. Data Sources

The Fengyun-3 (FY-3) satellite is China's second-generation polar-orbiting meteorological satellite. Compared to the previous generation, Fengyun-1 (FY-1), the FY-3 has made significant advancements and improvements in the accuracy of numerical weather forecasting products. The FY-3 satellite can conduct all-weather, multi-spectral, three-dimensional observations, monitoring global atmospheric and geophysical elements, providing satellite observation data for medium-term numerical weather forecasting, and monitoring ecological environments and large-scale natural disasters. Furthermore, the FY-3 satellite can provide satellite meteorological information for global environmental change, climate change research, and sectors such as oceanography, agriculture, forestry, aviation, and military applications [15].

China's Fengyun polar-orbiting meteorological satellites include the first generation (Fengyun-1C and 1D) and the second generation (Fengyun-3A to E, totaling five satellites), which have successively monitored the distribution and changes of Arctic sea ice. The detection instruments have evolved from visible infrared scanning radiometers to passive microwave radiometers and radar scatterometers (active), with observation spatial resolution improving from 25 km to 250 m. With dual satellites observing simultaneously, there can be nearly 15 high-frequency overpasses per day north of 85° north, enabling real-time and accurate capture of dynamic changes in Arctic sea ice, and providing monitoring products such as sea ice distribution, sea ice concentration, and sea ice type.



Figure 1. Physical image of FY-3D meteorological satellite.



Figure 2. Physical image of MERSI.

The FY-3D satellite, as shown in Figure 1, is equipped with the MERSI (Medium Resolution Spectral Imager), which has always been one of the core payloads of the FY-3 meteorological satellites, developed by the Shanghai Institute of Technical Physics, Chinese Academy of Sciences, as shown in Figure 2. In the FY-3 satellites, the A, B, and C satellites are equipped with the first generation of MERSI, which has a total of 20 channels. The MERSI-II onboard the FY-3D sat-

ellite increases the number of channels to 25 while maintaining the same imaging geometry as the first generation of MERSI. This includes 16 visible-near-infrared channels, 3 shortwave infrared channels, and 6 mid-to-long-wave infrared channels. Among these 25 channels, 6 channels have a ground resolution of 250 m, while the other 19 channels have a ground resolution of 1,000 m.

According to the “Meteorological Satellite Data Classification (QX/T 158-2012)”, the National Satellite Meteorological Center categorizes Fengyun meteorological satellite data into five levels, as described in Table 1. Among these, Level 0 data are raw data and are not open to external access [16]. Levels 1, 2, and 3 data are considered basic data and are available for user sharing. Users can search and download data through the Fengyun Satellite Remote Sensing Data Service website of the National Satellite Meteorological Center (<http://satellite.nsmc.org.cn>). According to Table 1, Levels 2 to 4 are classified as product-level data. Therefore, we can select the Level 1 data of MERSI-II as the foundational data source for Arctic sea ice monitoring.

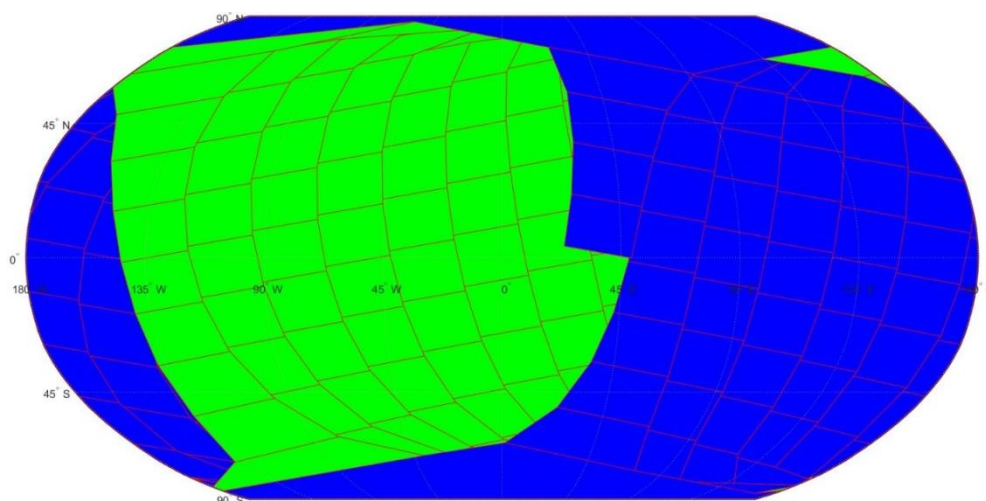


Figure 3. Coverage of MERSI-II data at 250 m resolution from Fengyun-3D Satellite.

Table 1. Classification of Fengyun meteorological satellite data.

Data Level	Abbreviation	Classification Principle
Level 0	L0	Raw satellite data received by the ground system
Level 1	L1	Basic data obtained from Level 0 data after quality inspection, image positioning, and radiometric calibration
Level 2	L2	Various application data obtained from Level 1 data through projection transformation, inversion, or other calculations
Level 3	L3	Statistical data obtained from Level 2 data through time averaging, accumulation, or analysis data obtained through human-computer interaction
Level 4	L4	Reanalysis data generated using Level 2 or Level 3 data and various weather and climate model products

To examine the coverage of MERSI-II data, we selected data with a resolution of 250 m, with each scene being acquired every 5 min from the remote sensing data service website. We extracted the latitude and longitude coordinates of the four corners of each image and used MATLAB to plot the trajectory, as shown in Figure 3. This clearly presents the coverage of MERSI-II data, illustrating that 288 scenes per day cover the global region at least once. By setting the latitude and longitude range, we can select images of interest, preprocess them, and extract sea ice data [17].

2.2. Model or Algorithm

Optical remote sensing is a method that utilizes the reflection, absorption, and scattering characteristics of electromagnetic waves in the visible and infrared bands to extract sea ice information. Common methods for extracting sea ice from optical remote sensing data include threshold-based methods, ratio methods, comparison methods, and feature extraction methods. The threshold-based method for sea ice extraction distinguishes sea ice from other land cover types by setting appropriate thresholds, based on the reflection characteristics of sea ice in the visible and infrared bands. The ratio method differentiates sea ice from other land cover types by calculating the ratios or normalized indices of different bands, such as using the NDVI (Normalized Difference Vegetation Index) to extract sea ice. The comparison method utilizes multi-temporal remote sensing images for comparison, extracting information based on changes in sea ice, such as determining sea ice areas by comparing images from two different times. Finally, the feature extraction method extracts characteristics such as shape and texture of sea ice, employing techniques like image segmentation and object recognition. When performing sea ice extraction, it is essential to consider data quality and preprocessing, as optical remote sensing data may be affected by weather conditions like clouds and fog. Additionally, different methods are suitable for different regions and seasons, so appropriate methods should be selected based on specific circumstances.

2.3. Key Steps and Methods

2.3.1. MERSI Data Preprocessing

To ensure the spatial consistency and comparability of pixel values in the multi-temporal and multi-band data from the Fengyun-3 meteorological satellite MERSI during processing, necessary preprocessing of the MERSI images from different time periods is required. This includes radiometric calibration to eliminate brightness differences between images taken at different times and bands; geometric correction to rectify any geometric distortions; image registration to align images from different time periods in spatial position; and image cropping to remove irrelevant information or extract areas of interest for subsequent processing and analysis. Through these four

key steps, MERSI data can be effectively processed, ensuring data quality and providing a reliable foundation for further analysis and applications.

(i). Radiometric Calibration

MERSI-II Level 1 data store the original observed pixel gray values as unsigned integers, which are output as DN* after multi-pixel normalization correction. To perform quantitative applications, these values need to be converted to reflectance through radiometric calibration. The dataset uses polynomial functions for calibration, with a third-degree calibration for infrared bands and a second-degree calibration for solar reflective bands. Before calibration, pixel corrections are necessary to adjust the DN* values for each channel, as shown in Eq. (1).

$$DN^{**} = slope * (DN^{*} - intercept) \quad (1)$$

where DN* represents the original pixel count values in the MERSI-II Level 1 dataset, and slope and intercept are the corresponding pixel correction coefficients for scaling and bias, stored in the MERSI-II Level 1 EV scientific dataset. The calibrated reflectance is derived from DN using Eq. (2).

$$Ref = k_2 * DN^2 + k_1 * DN + k_0 \quad (2)$$

where Ref is the calibrated reflectance in the visible spectrum, and k_0 , k_1 , k_2 are the calibration coefficients for the corresponding channels, stored in the first, second, and third columns of the VIS_Cal_Coeff scientific dataset of MERSI-II Level 1. Based on this, the conversion relationships for calibrated reflectance, radiance, and apparent reflectance are established, allowing the calculation of the apparent reflectance for the corresponding channels, as shown in the following equations.

$$Ref = \pi * \frac{L_{toa}}{E_0} \quad (3)$$

$$\rho = \frac{\pi * L_{toa} * d_{ES}^2}{E_0 * \cos \theta} = \frac{Ref * d_{ES}^2}{\cos \theta} \quad (4)$$

where L_{toa} is the radiance, E_0 is the solar irradiance, and d_{ES}^2 is the average distance from the Earth to the Sun, which can be considered constant and is obtained from the “Earth-Sun Distance Ratio” attributed in the MERSI-II Level 1 dataset. θ is the solar zenith angle.

(ii). Geometric Correction

MERSI-II is a multispectral imaging instrument that conducts Earth observations using 10-channel (1,000 m) and 40-channel (250 m) multi-pixel scanning. However, during imaging, factors such as geometric characteristics, Earth's surface curvature, topographical variations, and satellite mo-

tion jitter can cause geometric distortions. Therefore, geometric correction is necessary before applying the radiometrically corrected data in subsequent research. The MERSI-II Level 1 data include longitude and latitude information for each pixel, which can be utilized for geometric correction.

The GLT (Geographic Location Table) geometric correction method is a commonly used approach for geometric correction of MERSI-II Level 1 data. By generating a GLT (Geographic Location Lookup Table) from the existing latitude and longitude data, this table records the geographic location of each pixel in the corrected image. The two bands of the GLT represent the rows and columns of the corrected image, while the pixel gray values indicate the geographic coordinates corresponding to each pixel in the original image. This information is stored as signed integers, with positive values indicating the use of actual pixel position values and negative values indicating the use of adjacent pixel position values.

Since the research area is located in the high-latitude polar region, and the images obtained by polar orbiting satellites have different orientations, it is necessary to project the corrected images from geographic coordinates to the corresponding planar coordinates on the map. Here, polar azimuthal projection is used for re-projection, characterized by meridians as radial lines and parallels as concentric circles. The calculation formulas include a series of parameters such as reference latitude, reference longitude, the eccentricity of the Earth's ellipsoid, and the semi-major axis. To minimize deformation in the ice areas of the study region, the central latitude and longitude of the study area are generally chosen as the reference coordinates, and the WGS-84 ellipsoid model is used for calculations. The final re-projection calculation formulas include several parameters and computational steps.

In summary, performing geometric correction on MERSI-II Level 1 data is a prerequisite for subsequent application studies, and the GLT geometric correction method combined with polar azimuthal projection is commonly used method. These methods effectively address geometric distortions and convert the corrected data into planar coordinates on the map.

(iii). Image Registration

To conduct short-term predictions of independent sea ice movement, a time series dataset based on Fengyun-3 MERSI-II Level 1 data must be constructed. During the preprocessing of the raw data and the construction of the dataset, inter-channel registration and geometric registration must be performed to ensure that the pixels in the images at each moment in the time series correspond exactly to the actual geographic locations. Through geometric correction, the positional consistency of corresponding points between channels is already quite high; therefore, this study uses ENVI (The Environment for Visualizing Images) software to perform geometric registration on images from different times, employing a second-degree polynomial model and using bicubic convolution for resampling.

(iv). Image Cropping

To monitor sea ice movement and changes, all images are cropped to extract the maximum rectangular area of overlap after geometric correction and registration, considering the different imaging conditions and geometric distortions of each temporal image. This ensures that the images have a consistent coverage area, providing a unified foundation for the analysis of sea ice movement and changes.

2.3.2. Characteristics of Sea Ice in the Visible Spectrum

The reflective characteristics of sea ice in the visible and near-infrared bands are the most important basis for sea ice identification. Ice reflects significantly more in the visible spectrum than in the near-infrared spectrum, with reflectance for ice typically ranging from 0.35 to 0.65 in the visible spectrum, and additional ice containing bubbles can reach as high as 0.7 to 0.8, while the near-infrared reflectance is only about 0.2 [18]. Figure 4 shows the reflectance curves for ice, clouds, and water in two different areas of the Bering Sea, derived from statistical analysis of the MAS (MODIS Airborne Simulator) data across various bands. Snow-covered ice, new ice, and clouds exhibit significantly higher reflectance in the visible spectrum compared to water, which has reflectance below 0.2. Additionally, the reflectance of snow-covered ice and clouds shows relatively stable variation in the range of 0.5 to 0.7 μm , while the reflectance of new ice and water gradually decreases within this wavelength range. However, in the shortwave infrared band of 1.55 to 1.75 μm , there are significant differences in reflectance among snow-covered ice, new ice, and clouds. In this spectral range, clouds reflect solar radiation strongly, while ice absorbs solar radiation, resulting in a reflectance that is significantly lower than that of clouds.

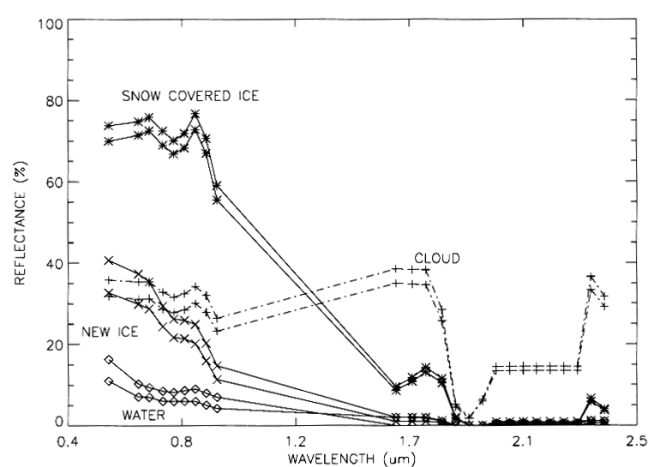


Figure 4. Reflectance curves for ice, clouds, and water in the Bering Sea region based on statistical analysis of MAS data for each band [19].

2.3.3. MERSI Data Method for Sea Ice Identification

Sea ice identification is the process of using image processing technology to distinguish sea ice from other land features, such as land, seawater, and clouds. In the Arctic region, the types of land features are relatively few, mainly including rocks, ice and snow on land, sea ice, and seawater. Additionally, clouds can interfere with the extraction of ice and snow pixels, making accurate sea ice identification particularly important. To achieve effective identification of sea ice, we can utilize the spectral characteristics of sea ice in the visible and near-infrared bands. By establishing a sea ice identification model, we can separate sea ice from other land

features, thereby obtaining information on the distribution of sea ice.

Specifically, the sea ice identification model processes the image to remove information related to land, clouds, and seawater, retaining only the sea ice pixels (as shown in Figure 5). This processing step effectively captures the distribution information of sea ice, laying the groundwork for subsequent monitoring and research. In summary, sea ice identification relies on image processing technology and its models to accurately distinguish and obtain information on the distribution of sea ice [20].

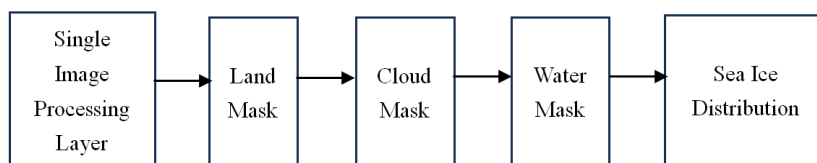


Figure 5. Sea ice identification model.

First, to simplify the process of extracting sea ice information and reduce interference, land masking is necessary. Since most areas within the Arctic Circle are covered by ice and snow, the variation in land information is limited, and the land mask can effectively improve the accuracy of sea ice information. With the support of GIS technology and ENVI image processing software, a land mask image with a spatial resolution of 250m was generated using the land-sea template dataset from MERSI Level 1 data with a spatial resolution of 1000m, combined with visual interpretation methods. The land mask for the Fram Strait (76°N–84°N, 30°W–15°E) is shown in Figure 6.



Figure 6. Land mask (green = land, white = other).

Next, by applying the land mask, we can successfully remove the land portion from the original image, retaining only the sea surface information. This step lays the foundation for subsequent sea ice identification, as shown in Figure 7.

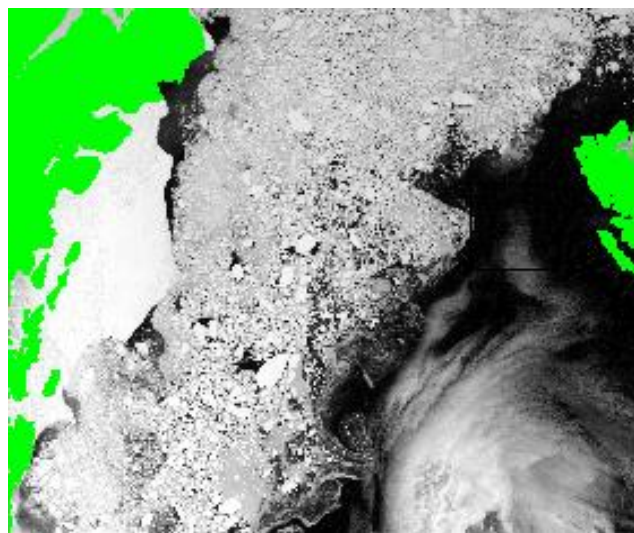


Figure 7. Result of applying the land mask.

After completing the land masking process, we further identify clouds. Clouds are another major factor affecting sea ice extraction. Using the Normalized Difference Snow Index (NDSI) and the reflectance from the sixth channel of MERSI as indicators for cloud identification, we employ a thresholding method to determine the optimal threshold. The identified cloud pixels are set as the background, generating a cloud mask image (as shown in Figure 8).



Figure 8. Cloud mask image (red = cloud, white = other).

After the cloud masking process, the land and clouds in the image are removed, leaving only the sea ice and seawater information, as shown in Figure 9.

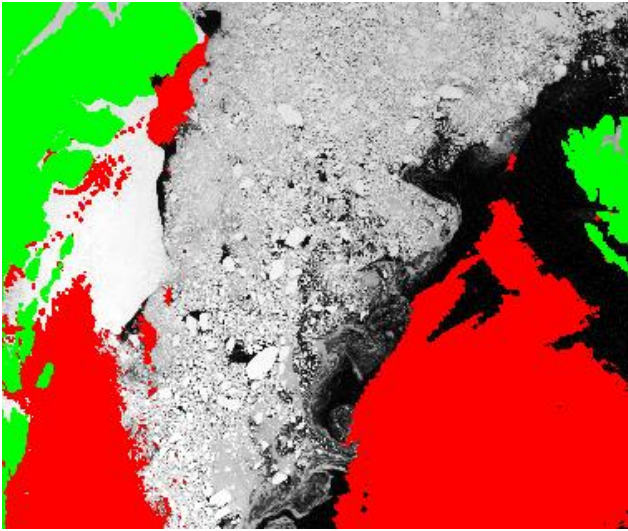


Figure 9. Result of applying the land and cloud masks.

It is important to note that the position and extent of clouds can change with each image, so it is necessary to find the optimal threshold for segmentation based on the grayscale information of each image. After completing the cloud masking, the next step is to perform seawater masking. Using the bands from MERSI channels 1 to 4, the reflectance of seawater is significantly lower than that of various types of sea ice. By dividing the reflectance images of MERSI channels 1 and 2 to obtain a ratio image, we can amplify the reflectance differences between seawater and sea ice in the visible spectrum, facilitating accurate identification of seawater. Based on criterion (5), the maximum inter-class variance thresholding method is used to determine the segmenta-

tion thresholds for the ratio image, as well as the reflectance images of MERSI channels 3 and 4, to identify seawater pixels in the image. The grayscale value of seawater pixels is set to 0, while the grayscale values of other pixels are set to 1, generating a seawater mask image (as shown in Figure 10).

$$\begin{cases} \rho_1 / \rho_2 > th3 \\ \rho_3 < th4 \\ \rho_4 < th5 \end{cases} \quad (5)$$

In this context, ρ_1 , ρ_2 , ρ_3 , ρ_4 , represent the reflectance of MERSI channels 1, 2, 3, and 4, respectively, while $th1$, $th2$, and $th3$ are the segmentation thresholds. Pixels that meet the discrimination criteria are considered as seawater pixels.

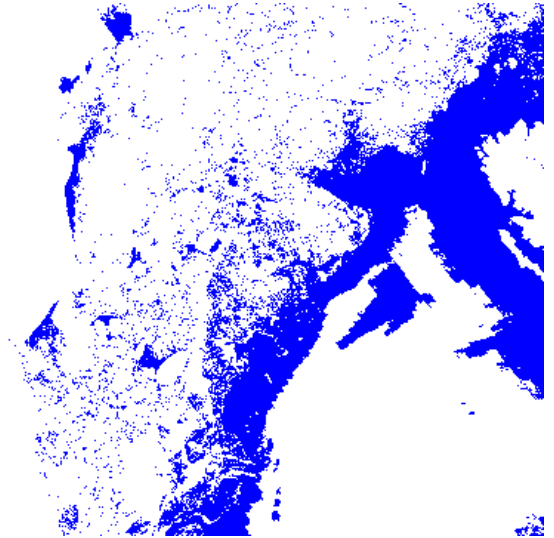


Figure 10. Seawater mask image (blue = seawater, white = other).

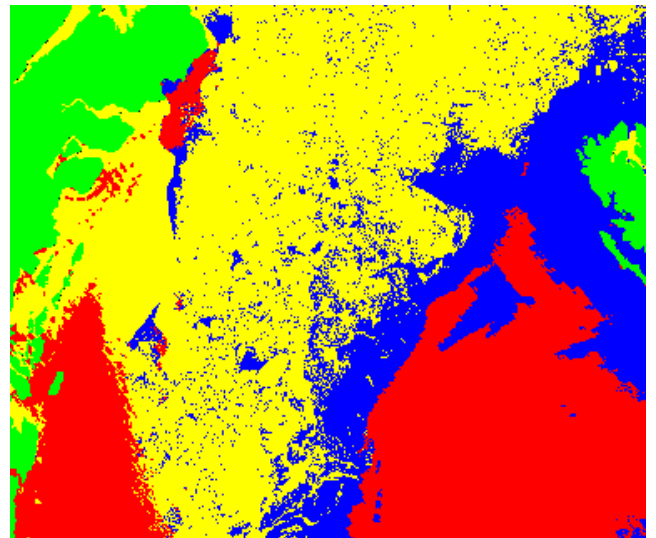


Figure 11. Ice identification results.

By applying the land, cloud, and seawater masks, we ultimately succeeded in removing the seawater information from the image while retaining the sea ice information, completing the entire sea ice identification process. The final identification results are shown in Figure 11. Through this series of processing steps, we can effectively extract the distribution information of sea ice, providing important data support for subsequent sea ice monitoring and research.

3. Conclusion and Outlook

The MERSI (FY-3/MERSI-II) onboard the Fengyun-3 meteorological satellite has a large scanning range and a short observation period, allowing it to obtain multiple observations of the same region in the polar areas within a single day. Additionally, FY-3/MERSI-II features high spatial resolution, which provides a significant advantage in monitoring the movement and changes of sea ice in the Arctic Ocean. To utilize FY-3/MERSI-II for sea ice identification, the spectral characteristics of sea ice, clouds, and seawater in the visible and near-infrared bands can be exploited. By establishing a sea ice identification model, the maximum interclass variance threshold method can be employed to automatically find the optimal segmentation threshold. This approach can reduce the impact of thin clouds on sea ice identification while preserving more sea ice pixels, thereby allowing for a more accurate identification of seawater and sea ice pixels in ice-water mixed regions and retaining detailed information about sea ice distribution.

By leveraging the observational data from FY-3/MERSI-II and the sea ice identification model, it is possible to monitor the movement and changes of sea ice in the Arctic Ocean and obtain detailed information about sea ice. This is of significant importance for studying the evolution process of sea ice, predicting future changes in sea ice, and assessing the response of sea ice to climate change.

In the harsh weather conditions of the Arctic region, the use of visible and near-infrared band data from FY-3/MERSI-II for sea ice observation can be affected by clouds and fog. Although various algorithms have been considered for extracting targets like sea ice under thin clouds, there remains no perfect solution when the cloud cover is complete. Therefore, future research could combine data from other bands, such as thermal infrared and microwave, to take advantage of the characteristics of each band and enhance the applicability of the algorithms. By integrating data from multiple bands, it is possible to offset the limitations of the visible and near-infrared bands in cloudy conditions. The thermal infrared band can identify sea ice by detecting the thermal radiation of target objects, while the microwave band can penetrate cloud cover to obtain information about sea ice. The comprehensive use of these band data can improve the observation accuracy and precision of sea ice. Moreover, other observation methods and technologies could be considered to enhance sea ice observation capabilities. For example, combining

satellite remote sensing data with technologies such as Lidar can provide a more comprehensive and accurate understanding of sea ice. Additionally, strengthening the detection and identification capabilities of clouds and fog would facilitate better extraction of information about sea ice and other target objects. In summary, by integrating data from multiple bands and utilizing other observation methods, the ability to observe sea ice can be further improved, effectively addressing the observational challenges posed by cloudy and foggy weather.

Subsequently, after extracting the overall distribution of sea ice, methods such as regional double-peak threshold segmentation combined with gradient difference, or leveraging the advantages of convolutional neural networks and recurrent neural networks, could be employed to achieve refined identification of independent sea ice in the Arctic seas and short-term predictions of independent sea ice movement. Based on the results of sea ice identification and independent ice extraction, the study has acquired parameters including sea ice density, size, and shape in the demonstration area. Using the sea ice movement tracking method based on the matching of independent ice with the same name, the speed of each independent ice block was calculated. By analyzing the differences in movement speeds between independent ice blocks, a more comprehensive and detailed analysis of sea ice movement characteristics and the correlation between sea ice movement and sea ice feature parameters can be achieved.

Abbreviations

FY-3	Fengyun-3
MERSI	Medium Resolution Spectral Imager
NDSI	Normalized Difference Snow Index
NDVI	Normalized Difference Vegetation Index
SAR	Synthetic Aperture Radar
SSM/I	Special Sensor Microwave/Imager
AMSR-2	Advanced Microwave Scanning Radiometer-2
NSIDC	National Snow and Ice Data Center
IFREMER	French Research Institute for the Exploitation of the Seas
OSI-SAF	Ocean and Sea Ice Satellite Application Facility
GIS	Geographic Information System
L0	Level 0
L1	Level 1
L2	Level 2
L3	Level 3
L4	Level 4
EV	Earth View

Author Contributions

Chun Shen: Conceptualization, Investigation, Supervision, Validation

Conflicts of Interest

The authors declare that there are no conflicts of interest regarding the publication of this paper.

References

- [1] Andrews, J., Babb, D., & Barber, D. G. (2018). Climate change and sea ice: Shipping in Hudson Bay, Hudson Strait, and Foxe Basin (1980–2016). *Elementa: Science of the Anthropocene*, 6, 19. <https://doi.org/10.1525/elementa.281>
- [2] Kiiski, T. (2017). Feasibility of Commercial Cargo Shipping along the Northern Sea Route. <https://urn.fi/URN:ISBN:978-951-29-6691-2>
- [3] Zhang, W., Wang, Y., Mou, C. R., et al. (2024). Route planning for the Arctic Northeast Passage considering multiple risk factors. *Journal of Dalian Maritime University*, 50(02), 1-10. <https://doi.org/10.16411/j.cnki.issn1006-7736.2024.02.001>
- [4] Lan, Q., & Zhang, X. (2024). Development of the Arctic route under the Belt and Road Initiative: Drivers, trends, and China's response. *Journal of Beijing Jiaotong University (Social Sciences Edition)*, 1-15. [2024-09-26]. <https://doi.org/10.16797/j.cnki.11-5224/c.20240729.010>
- [5] Wang, H., Li, Z., Li, C., et al. (2024). Opportunities, challenges, and responses for China regarding the construction of the Arctic route. *International Economic Cooperation*, 40(04), 67-76+94. <https://doi.org/10.20090/j.cnki.gjjh.2024.4.7>
- [6] Fang, Y., Wang, X., Chen, Z. Q., et al. (2023). Analysis of summer sea ice drift and changes in the Fram Strait from 2011 to 2020. *Acta Geophysica*, 66(07), 2726-2740.
- [7] Liang, S. (2021). Research on remote sensing inversion methods for polar sea ice density and thickness. University of Chinese Academy of Sciences (Institute of Space Information Innovation, Chinese Academy of Sciences). <https://doi.org/10.44231/d.cnki.gktxc.2021.000018>
- [8] Yan, Q., & Huang, W. (2019). Sea Ice Remote Sensing Using GNSS-R: A Review. *Remote Sens.* 11, 2565. <https://doi.org/10.3390/rs11212565>
- [9] Zhang, X., Fang, H. L., Wang, R. F., et al. (2024). Inversion method for Arctic thin ice thickness based on FY-3D microwave imager. *Advances in Marine Science*, 1-13. [2024-09-26]. <http://kns.cnki.net/kcms/detail/37.1387.P.20240604.0956.002.html>
- [10] Zheng, M. W., Li, X. M., & Ren, Y. Z. (2018). Research on automatic detection methods for polar sea ice using Synthetic Aperture Radar from GaoFen-3. *Acta Oceanologica Sinica*, 40(09), 113-124.
- [11] Zhao, C. F., Xu, R., & Zhao, K. (2019). Research on polar sea ice detection methods based on HY-2A/SCAT data. *Journal of Ocean University of China (Natural Science Edition)*, 49(10), 140-149. <https://doi.org/10.16441/j.cnki.hdxh.20190275>
- [12] Kharbouche, S., & Muller, J.P. (2019). Sea Ice Albedo from MISR and MODIS: Production, Validation, and Trend Analysis. *Remote Sensing*, 11(1), 9. <https://doi.org/10.3390/rs11010009>
- [13] Zhou, Y., Kuang, D. B., & Gong, C. L., et al. (2017). Method for extracting Arctic sea ice parameters from MERSI images of Fengyun-3 satellite. *Journal of Infrared and Millimeter Waves*, 36(01), 41-48+126-127.
- [14] Yang, Z. J., Wang, Z. M., & Liu, T. T. (2023). Accuracy assessment of estimating Arctic sea ice area and edge using microwave data from Fengyun-3D. *Polar Research*, 35(01), 46-58. <https://doi.org/10.13679/j.jdyj.20210093>
- [15] Miao, S. X., Sun, K. M., Hu, X. Q., et al. (2024). Analysis of monitoring capabilities for plateau lake range based on MER-SI-II images from Fengyun-3D. *Journal of Wuhan University (Information Science Edition)*, 1-15. [2024-08-18]. <https://doi.org/10.13203/j.whugis20220653>
- [16] China Meteorological Administration. (2018). [Online]. Available: https://www.cma.gov.cn/zfxgk/gknr/wjgk/gfxwj/201808/t20180820_1711977.html
- [17] Zhang, J. W., & Qiu, Z. F. (2021). Quality assessment of FY-3D MERSI II data for oceanic water areas. *Acta Optica Sinica*, 41(12), 19-38.
- [18] Zhu, X. Y., Su, J., Song, M., et al. (2022). Optimization of the algorithm for retrieving ice thickness in the Bohai Sea based on MODIS data. *Acta Oceanologica Sinica*, 44(12), 70-83.
- [19] Riggs, G. A., Hall, D. K., & Ackerman, S. A. (1999). Sea ice extent and classification mapping with the Moderate Resolution Imaging Spectroradiometer Airborne Simulator. *Remote Sensing of Environment*, 68(2), 152-163.
- [20] Zheng, F. Q., Kuang, D. B., Hu, Y., et al. (2022). Prediction of independent sea ice motion in the Arctic channel based on Multiloss-SAM-ConvLSTM. *Journal of Infrared and Millimeter Waves*, 41(5), 894-904.